


Communication

Switch-on Fluorescence Analysis of Protease Activity with the Assistance of a Nickel Ion-Nitrilotriacetic Acid-Conjugated Magnetic Nanoparticle

Xiaohua Ma ¹, Yingxin Lv ², Panpan Liu ², Yuanqiang Hao ^{1,*} and Ning Xia ^{2,*} 

¹ Henan Key Laboratory of Biomolecular Recognition and Sensing, Shangqiu Normal University, Shangqiu 476000, China

² College of Chemistry and Chemical Engineering, Anyang Normal University, Anyang 455000, China

* Correspondence: haoyuanqiang@aliyun.com (Y.H.); ningxia@aynu.edu.cn (N.X.)

Abstract: Heterogeneous protease biosensors show high sensitivity and selectivity but usually require the immobilization of peptide substrates on a solid interface. Such methods exhibit the disadvantages of complex immobilization steps and low enzymatic efficiency induced by steric hindrance. In this work, we proposed an immobilization-free strategy for protease detection with high simplicity, sensitivity and selectivity. Specifically, a single-labeled peptide with oligohistidine-tag (His-tag) was designed as the protease substrate, which can be captured by a nickel ion-nitrilotriacetic acid (Ni-NTA)-conjugated magnetic nanoparticle (MNP) through the coordination interaction between His-tag and Ni-NTA. When the peptide was digested by protease in a homogeneous solution, the signal-labeled segment was released from the substrate. The unreacted peptide substrates could be removed by Ni-NTA-MNP, and the released segments remained in solution to emit strong fluorescence. The method was used to determine protease of caspase-3 with a low detection limit (4 pg/mL). By changing the peptide sequence and signal reporters, the proposal could be used to develop novel homogeneous biosensors for the detection of other proteases.

Keywords: proteases; caspase-3; nitrilotriacetic acid; homogeneous assays; fluorescence; magnetic nanoparticle



Citation: Ma, X.; Lv, Y.; Liu, P.; Hao, Y.; Xia, N. Switch-on Fluorescence Analysis of Protease Activity with the Assistance of a Nickel Ion-Nitrilotriacetic Acid-Conjugated Magnetic Nanoparticle. *Molecules* **2023**, *28*, 3426. <https://doi.org/10.3390/molecules28083426>

Academic Editor: Takuya Terai

Received: 8 March 2023

Revised: 7 April 2023

Accepted: 10 April 2023

Published: 13 April 2023



Copyright: © 2023 by the authors. Licensee MDPI, Basel, Switzerland. This article is an open access article distributed under the terms and conditions of the Creative Commons Attribution (CC BY) license (<https://creativecommons.org/licenses/by/4.0/>).

1. Introduction

Proteases participate in many important physiological processes, such as protein digestion, blood coagulation, and immune system activation. The occurrence of some diseases is closely related to the abnormal activity of proteases [1–5]. For example, matrix metalloproteinases are overexpressed in some cancers, serine proteases are involved in the closely coordinated coagulation cascade, human immunodeficiency virus (HIV) proteases are overexpressed in the life cycle of HIV patients, SARS-CoV-2 main proteases are related to COVID-19, and β / γ -secretases are responsible for the production of toxic β -amyloid peptides in the brains of patients with Alzheimer's disease. Some diseases can be treated well by regulating the activity of proteases with inhibitor drugs. Therefore, the development of simple, sensitive, low cost, and high-throughput methods for monitoring protease activity is of great significance for early diagnosis and effective treatment of protease-related diseases.

Proteases can catalyze the hydrolysis of proteins or peptides and decompose them into amino acids or small peptide fragments. The methods for analysis of protease activity usually include homogenous and heterogeneous assays, such as liquid chromatography, mass spectrometry, electrochemistry, colorimetry, fluorescence, surface plasmon resonance and so on [4,6–17]. Among these, fluorescence-based homogenous analysis is the most commonly used method for protease detection because of its high sensitivity and quantitative results. In this method, the substrate peptide is often modified with a pair of quencher

and fluorophore groups [18–23]. The hydrolysis of peptides can lead to the separation of quenchers and fluorophores, leading to the increase in the fluorescence signal. Although this fluorescence method has the characteristics of high sensitivity and selectivity, dual-labeling of peptides at both terminals may increase the cost and complexity of substrate synthesis, limit the protease to approach the cleavage site and reduce the cleavage efficiency of proteolysis [24–28]. Recently, single-labeled fluorescent nucleotide probes have been widely used for the detection of metal ions and nucleic acids with the advantages of low cost and high sensitivity [29,30]. However, there are few reports on the general detection of protease activity using single-labeled peptide substrates [31].

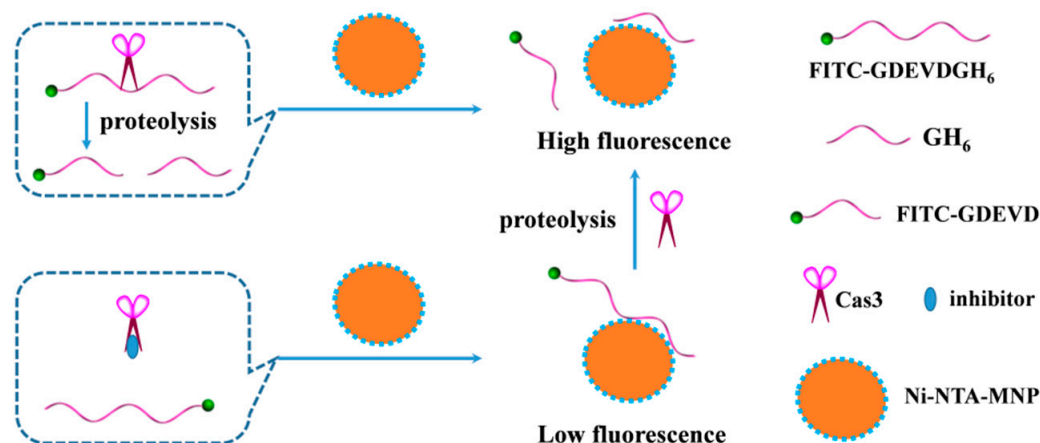
Nanomaterials such as gold nanoparticles, carbon nanotubes and graphene oxide as quenchers have been integrated with single-labeled fluorescent peptides for monitoring protease activity through the fluorescence resonance energy transfer (FRET) effect [32–37]. The nanomaterials usually exhibit superior quenching ability to molecular quenchers due to the long-range energy transfer. However, immobilization of peptide substrates on the solid surface may cause the steric hindrance effect to affect the configurational freedom of peptides, thus limiting their interaction with proteases and decreasing the cleavage efficiency [38,39]. In addition, peptide immobilization requires laborious and time-consuming procedures. In this respect, it is of paramount importance to the manipulation of external surfaces for anchoring peptide substrates. Oligohistidine-tag (His-tag) can be easily integrated into peptides or proteins through synthetic or recombinant techniques. The nickel ion-nitrilotriacetic acid (Ni-NTA) complex shows high-affinity toward His-tag in which four coordination sites are occupied by NTA and two of them are coordinated with two imidazole moieties of His-tag [40–42]. Based on strong and specific interactions, Ni-NTA-conjugated polymers, magnetic beads and silica nanoparticles have been widely applied for the separation, purification and delivery of peptides and proteins with His-tags [41,43–46]. In this work, the commercialized Ni-NTA-conjugated magnetic nanoparticles (MNPs) were employed for the development of a switch-on fluorescent biosensor for monitoring protease activity with Caspase-3 (Cas3) as an example. Fluorescently-labeled peptide substrates with His-tags can be captured by Ni-NTA-MNPs through the interactions between His-tag and Ni-NTA, leading to a decrease in fluorescence. When peptide substrates were degraded using the proteolysis, the fluorophore-included peptide segments were released from the peptide substrates or the peptide-conjugated NTA-Ni-MNPs, thus turning on the fluorescence of solution. The reaction rate of proteolysis for the peptides dispersed in solution and immobilized on the surface of NTA-Ni-MNPs was investigated. This strategy can be used for the detection of various proteases by matching the peptide sequences specific to the targets. In addition, by replacing the fluorophores with other signal molecules such as electroactive molecules, enzymes and nanoparticles, single-labeled peptides could be used for electrochemical or colorimetric analysis of the activity of various proteases.

2. Results and Discussion

2.1. Principle of This Proposal

Cas3, an important cysteine protease of the caspase family, plays a critical role in the cell apoptosis pathway [47,48]. To verify the analytical performances of this proposal, Cas3 was used as the model analyte. The principle of magnetically assisted assays of Cas3 is shown in Scheme 1. His-tag (HHHHHH or H₆) was included in the C-terminal of a Cas3-recognized peptide sequence (DEVD), and fluorescein isothiocyanate (FITC) was labeled in the N-terminal of the peptide. The peptide substrate of FITC-GDEVGH₆ could be captured and removed by Ni-NTA-MNP through the interaction between His-tag and Ni-NTA, thus quenching the fluorescence. Once the peptide was selectively digested by Cas3 in solution, the FITC-labeled segment (FITC-GDEV) was released from the substrate. The released segment could not be removed by Ni-NTA-MNP even under the magnetic force and thus emitted a strong fluorescence. Inhibiting the activity of Cas3 with a potential inhibitor could prevent the cleavage of the substrate peptide and thus cause the decrease in the fluorescence signal. The fluorescence intensity was proportional to the concentration

and activity of Cas3, allowing for the detection of Cas3 and screening of its inhibitor drugs. The strategy is simple and sensitive because it does not require the pre-immobilization of the peptide substrate on the solid surface, thus eliminating the steric hindrance effect and improving the cleavage efficiency.



Scheme 1. Schematic illustration of the method for Cas3 detection.

2.2. Feasibility for Cas3 Detection

Figure 1 shows the results to confirm the validity of the proposal. The fluorescence intensity of the peptide substrate decreased significantly after being incubated with Ni-NTA-MNP under a magnetic force (c.f. curves 1 and 2). The change was time-independent, indicating a rapid coordination interaction between His₆ tag and Ni-NTA. However, no obvious change in the fluorescence signal was observed when the H₆-free peptide (FITC-GDEVD) was incubated with Ni-NTA-MNP at the same condition. The results indicated that the peptide substrate was captured and removed by Ni-NTA-MNP through the interaction between His-tag and Ni-NTA. Interestingly, when the peptide substrate was incubated with Cas3 and then treated with Ni-NTA-MNP, the fluorescence signal increased greatly (curve 3). The result confirmed that the peptide probe could be enzymatically cleaved with Cas3, thus leaving the FITC-GDEVD segment in solution for determination. To evaluate the influence of steric hindrance on the cleavage efficiency, the FITC-GDEVDGH₆ substrates were immobilized on the Ni-NTA-MNP surface and then digested by Cas3 at the same experimental conditions. Consequently, the fluorescence intensity (curve 4) was lower than that achieved by the immobilization-free method (curve 3), suggesting that the immobilization of the peptide on the solid surface decreased the cleavage efficiency to some extent. The problem may be resolved by adding a spacer between the solid surface and the cleavage core of the peptide or by employing small-size nanoparticles to load the peptide substrate.

2.3. Optimization of Experimental Conditions

To obtain the best detection performances, the experimental conditions, including peptide concentration and enzymolysis time, were explored. Low background signal can favor the sensitivity of an analytical method. We first investigated the dependence of the fluorescence signal on the peptide concentration. It was found that the fluorescence signal was close to the background when the peptide concentration was below 1 μ M (Figure 2A). Beyond this value, the fluorescence intensity began to raise with the increase in peptide concentration. The signal began to increase, implying that the surface of Ni-NTA-MNP was saturated by the peptide probe. In this work, a compromising concentration of peptide was used in light of the real level of Cas3 in samples and the low signal-to-noise ratio. We also found that the fluorescence intensity increased and then reached a platform with the increase of enzymolysis time (Figure 2B). To achieve sensitive and rapid assays, 30 min was chosen as the reaction time for the cleavage event.

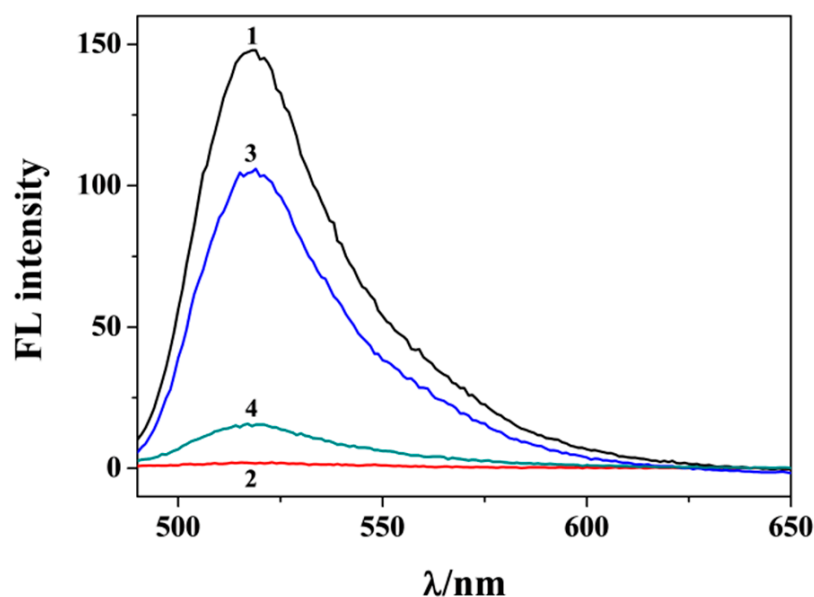


Figure 1. Fluorescence spectra of different systems: FITC-GDEVGDGH₆ (curve 1), FITC-GDEVGDGH₆ + Ni-NTA-MNP (curve 2) and FITC-GDEVGDGH₆/Cas3 + Ni-NTA-MNP (curve 3). Curve 4 corresponds to that of incubation of FITC-GDEVGDGH₆/Ni-NTA-MNP with Cas3. The concentrations of FITC-GDEVGDGH₆ and Cas3 used were 500 nM and 100 ng/mL.

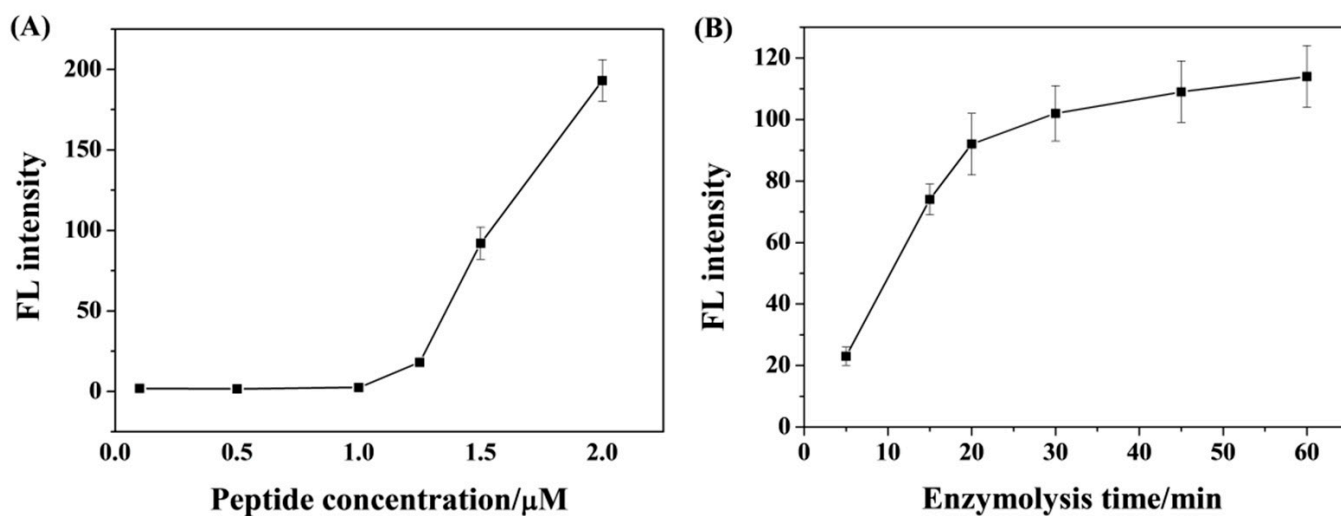


Figure 2. Dependence of fluorescence intensity on peptide concentration (A) and enzymolysis time (B).

2.4. Analytical Performances

Under optimal conditions, we investigated the analytical performances of this method by determining different concentrations of Cas3. As shown in Figure 3A, the fluorescence signal increased with the increase of Cas3 concentration. A good linear relationship between the fluorescence intensity and Cas3 concentration was found in the range of 0.01–25 ng/mL (Figure 3B). The linear equation is expressed as $F = 11.4 + 2.4[\text{Cas3}]$ (ng/mL). The limit of detection (LOD) was found to be 4 pg/mL, which is lower than that of other fluorescence assays with nanomaterials as the quenchers and carriers to load the peptide substrates (Table 1). The sensitivity is also comparable to that achieved by the heterogeneous methods through immobilization of peptides on a solid surface for enzymatic cleavage [49,50]. The high sensitivity should be attributed to the low background signal and high cleavage efficiency of this proposal.

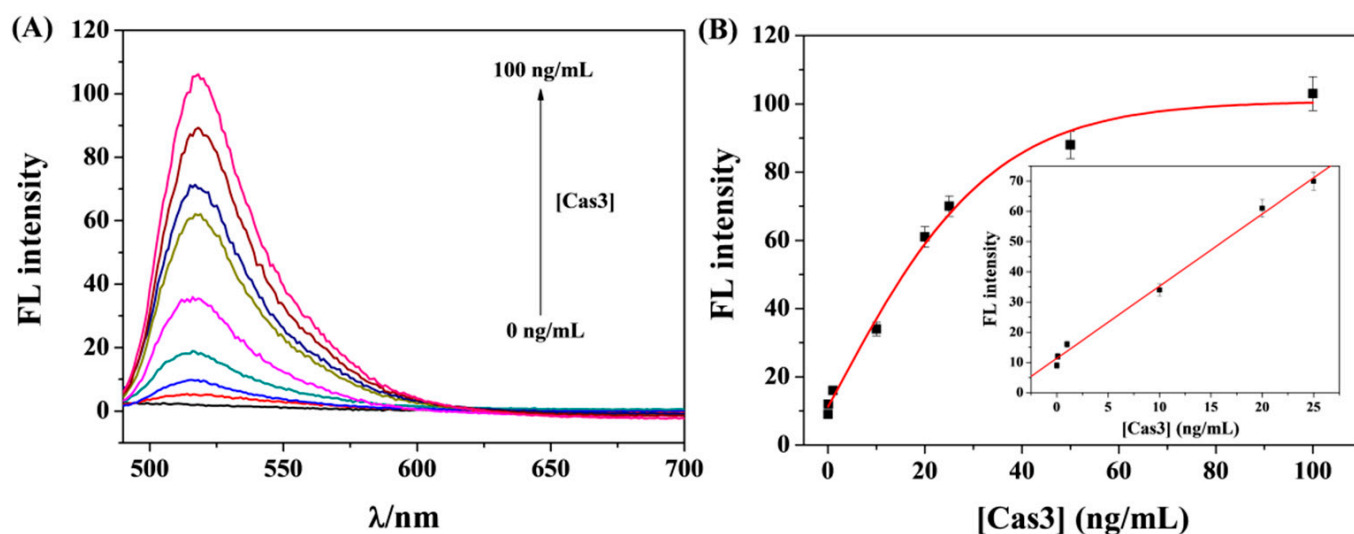


Figure 3. (A) Fluorescence spectra for the assays of various concentrations of Cas3 (from bottom to top: 0, 0.01, 0.1, 1, 10, 20, 25, 50 and 100 ng/mL). (B) Calibration curve between fluorescence intensity and Cas concentration.

Table 1. Analytical performances of nanomaterial-based fluorescence assays of Cas3.

Materials/Reporters	Linear Range	LOD	Ref.
AuNPs/dye	0–1 unit/mL	0.0079 unit/mL	[51]
AuNPs/dye	0–300 ng/mL	0.073 ng/mL	[52]
AuNPs/dye	3.2–100 pg/mL	1.3 pg/mL	[53]
AuNPs/SiNPs	0.05–1.0 U/mL	0.05 U/mL	[54]
GO/dye	7.25–362 ng/mL	7.25 ng/mL	[55]
GO/dye	2–360 ng/mL	0.33 ng/mL	[56]
qPNPs/dye	2–40 nM	0.09 nM	[57]
MCN/dye	0.01–1 ng/mL	0.4 pg/mL	[58]
MB/dye	0.01–25 ng/mL	4 pg/mL	This work

Abbreviations: AuNPs, gold nanoparticles; SiNPs, [Ru(bpy)₃]²⁺-encapsulated silica nanoparticles; GO, graphene oxide; qPNPs, polymeric nanoquenchers; MCN, mesoporous carbon nanospheres.

2.5. Selectivity

To explore the selectivity, a series of proteases were tested, including Cas3, thrombin, trypsin, β -secretase and PSA. As a result, only Cas3 caused the enhancement of fluorescence intensity (Figure 4A). Other proteases did not induce a significant signal change. The good selectivity of the proposal can be attributed to the high specificity of the peptide toward Cas3 and the unique interaction between His-tag and Ni-NTA. We also investigated the influence of other possible components in biological samples such as serum on the detection of Cas3. It was found that there is no significant difference in the signals for the assays of Cas3 in buffer and diluted serum. This result is acceptable since the commercialized Ni-NTA-MNPs were highly specific to His-tag peptides or proteins and only a few natural species with His-tag exist in serum at most.

To further confirm that the method is highly specific to active Cas3, the inhibition efficiency of a well-known inhibitor (DEVD-FMK) was evaluated. With the increase in inhibitor concentration, the fluorescence intensity decreased gradually and finally began to level off (Figure 4B). This demonstrated that the inhibitor prevented the cleavage of peptides by depressing the enzymatic activity of Cas3. Based on the relationship between fluorescence intensity and inhibitor concentration, the half-maximum inhibition value (IC₅₀) was found to be 4.6 nM for 20 ng/mL Cas3. The inhibition efficiency was in agreement with that evaluated by other methods [59–62], suggesting that the method has a promising application for rapid and high-throughput screening of protease inhibitors.

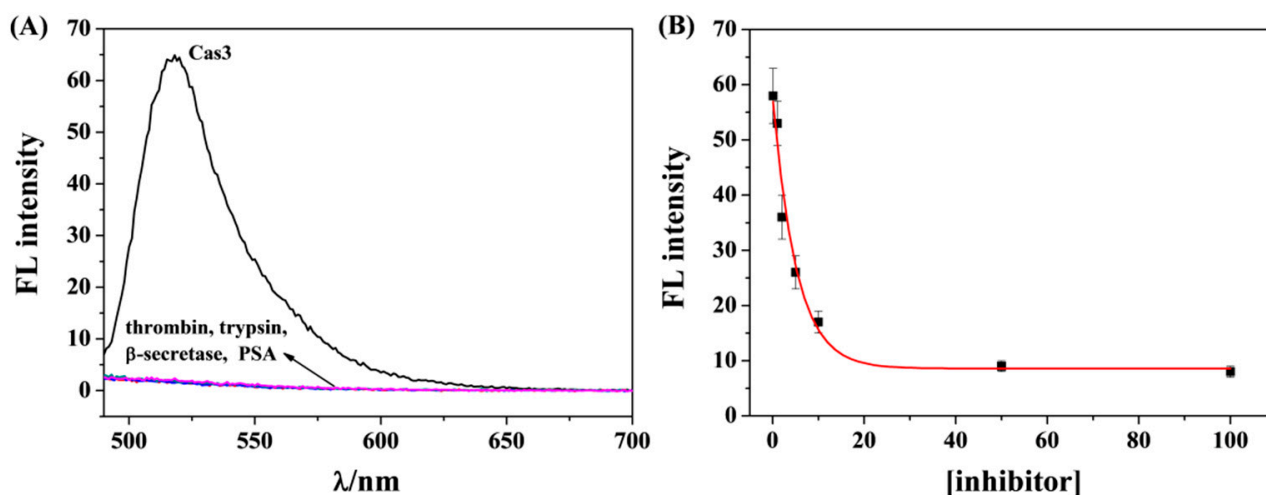


Figure 4. (A) Selectivity of this method toward 20 ng/mL Cas, thrombin, trypsin, β -secretase and PSA. (B) Dependence of fluorescence intensity on inhibitor concentration.

2.6. Evaluation of Cell Apoptosis

To indicate the applicability of this proposal, apoptosis was evaluated by monitoring the activity of Cas3 in the cell lysates. MCF-7 cells were induced to apoptosis with a classical inducer staurosporine. As shown in Figure 5, the fluorescence intensity was significantly intensified with an increasing number of cells induced with staurosporine. However, a slight change was observed for the assays of cells without treatment with the inducer. This result suggests that the level or activity of Cas3 in the apoptotic cells is higher than that in the living cells, which is consistent with that of previous reports [59,60]. Therefore, the proposed method could be used to determine Cas3 in biological samples and evaluate cell apoptosis, showing great potential for developing therapeutic drugs toward apoptosis-related diseases.

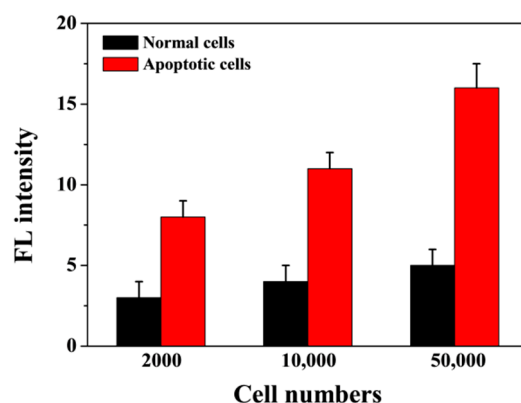


Figure 5. Results for the detection of Cas3 in the normal and apoptotic cells.

3. Experimental

3.1. Chemicals and Reagents

Cas3, β -secretase and thrombin were ordered from Sigma-Aldrich (Shanghai, China). Trypsin was provided by Sangon Biotech. Co., Ltd. (Shanghai, China). Prostate-specific antigen (PSA) was obtained from Linc-Bio Science Co., Ltd. (Shanghai, China). Peptides were synthesized with a solid phase synthesis method and purified using ChinaPeptides Co., Ltd. (Shanghai, China). NTA-Ni-MNPs with an average size of 400 nm were purchased from PuriMag Biotech. (Xiamen, China). Other reagents were of analytical grade and used without further purification. All the aqueous solutions were freshly prepared with ultrapure water treated with a Millipore system.

3.2. Procedures for Cas3 Detection

A total of 100 μ L of peptide substrate with the sequence of FITC-GDEVGDGHHHHH (denoted as FITC-GDEVGDG₆) was incubated with 100 μ L of Cas3 in phosphate buffer (10 mM, pH 7.4) at room temperature for a given time. Following this, 10 μ L of 12.5 mg/mL Ni-NTA-MNP suspension was added to the reaction solution and shaken for 5 min. Under the action of magnetic force, the supernatant solution was removed for fluorescence measurement on a fluorescence spectrometer with an excitation wavelength of 470 nm.

To evaluate the inhibition efficiency, the inhibitor was incubated with Cas3 for 10 min. Then, the mixture of Cas3 and inhibitor was incubated with the peptide substrate following the above procedure. The inhibition efficiency was calculated according to the change in fluorescence intensity.

3.3. Apoptosis Analysis

The extraction of cell lysates from living and apoptotic MCF-7 cells followed the procedure in our previous reports [59,60]. The collected lysates were diluted at different times with phosphate buffer and then analyzed with the steps as those for the assays of Cas3 standard samples.

4. Conclusions

In summary, a sensitive and simple homogeneous fluorescence method was proposed for the determination of proteases with Cas3 as the model analyte. The influence of steric hindrance on the enzymatic efficiency was also evaluated. Our proposal does not require the pre-immobilization of the peptide substrate, simplifying the operation steps and improving the sensitivity. The LOD of the method is lower than that of other fluorescence assays via immobilization of substrates on solid surfaces and comparable to that of heterogeneous strategies with signal amplifications of enzymes or nanomaterials. The method was successfully used to evaluate inhibition efficiency and monitor cell apoptosis. Other protease biosensors may be readily designed with this proposal by matching the sequence-specific peptide substrates and signal reporters.

Author Contributions: Conceptualization, Y.H.; methodology, X.M.; investigation, X.M., Y.L. and P.L.; writing—original draft preparation, X.M. and Y.H.; writing—review and editing, N.X.; project administration, Y.H.; funding acquisition, N.X. All authors have read and agreed to the published version of the manuscript.

Funding: This research was funded by the Program for Innovative Research Team of Science and Technology in the University of Henan Province (21IRTSTHN005) and the National Natural Science Foundation of China (22005185).

Institutional Review Board Statement: Not applicable.

Informed Consent Statement: Not applicable.

Data Availability Statement: Not applicable.

Conflicts of Interest: The authors declare no conflict of interest.

Sample Availability: Not applicable.

References

1. Poreba, M.; Szalek, A.; Kasperkiewicz, P.; Rut, W.; Salvesen, G.S.; Drag, M. Small molecule active site directed tools for studying human caspases. *Chem. Rev.* **2015**, *115*, 12546–12629. [[CrossRef](#)]
2. Rodriguez-Rios, M.; Megia-Fernandez, A.; Norman, D.J.; Bradley, M. Peptide probes for proteases—innovations and applications for monitoring proteolytic activity. *Chem. Soc. Rev.* **2022**, *51*, 2081–2120. [[CrossRef](#)] [[PubMed](#)]
3. Bąchor, R. Peptidyl-resin substrates as a tool in the analysis of caspase activity. *Molecules* **2022**, *27*, 4107. [[CrossRef](#)]
4. Eivazzadeh-Keihan, R.; Saadatidizaji, Z.; Maleki, A.; de la Guardia, M.; Mahdavi, M.; Barzegar, S.; Ahadian, S. Recent progresses in development of biosensors for thrombin detection. *Biosensors* **2022**, *12*, 767. [[CrossRef](#)] [[PubMed](#)]
5. Ullrich, S.; Nitsche, C. The SARS-CoV-2 main protease as drug target. *Bioorg. Med. Chem. Lett.* **2020**, *30*, 127377. [[CrossRef](#)] [[PubMed](#)]

6. Ong, I.L.H.; Yang, K.-L. Recent developments in protease activity assays and sensors. *Analyst* **2017**, *142*, 1867–1881. [[CrossRef](#)]
7. Kang, H.J.; Kim, J.H.; Chung, S.J. Homogeneous detection of caspase-3 using intrinsic fluorescence resonance energy transfer (iFRET). *Biosens. Bioelectron.* **2015**, *67*, 413–418. [[CrossRef](#)] [[PubMed](#)]
8. Yin, X.; Yang, B.; Chen, B.; He, M.; Hu, B. Multifunctional gold nanocluster decorated metal–organic framework for real-time monitoring of targeted drug delivery and quantitative evaluation of cellular therapeutic response. *Anal. Chem.* **2019**, *91*, 10596–10603. [[CrossRef](#)] [[PubMed](#)]
9. Liu, M.; Zhang, D.; Zhang, X.; Xu, Q.; Ma, F.; Zhang, C.-Y. Label-free and amplified detection of apoptosis-associated caspase activity using branched rolling circle amplification. *Chem. Commun.* **2020**, *56*, 5243–5246. [[CrossRef](#)] [[PubMed](#)]
10. Huang, X.; Liang, Y.; Ruan, L.; Ren, J. Chemiluminescent detection of cell apoptosis enzyme by gold nanoparticle-based resonance energy transfer assay. *Anal. Bioanal. Chem.* **2014**, *406*, 5677–5684. [[CrossRef](#)] [[PubMed](#)]
11. Munoz-San Martin, C.; Pedrero, M.; Gamella, M.; Montero-Calle, A.; Barderas, R.; Campuzano, S.; Pingarron, J.M. A novel peptide-based electrochemical biosensor for the determination of a metastasis-linked protease in pancreatic cancer cells. *Anal. Bioanal. Chem.* **2020**, *412*, 6177–6188. [[CrossRef](#)] [[PubMed](#)]
12. Zhang, J.; Qi, H.; Li, Z.; Zhang, N.; Gao, Q.; Zhang, C. Electrogenerated chemiluminescence bioanalytic system based on biocleavage of probes and homogeneous detection. *Anal. Chem.* **2015**, *87*, 6510–6515. [[CrossRef](#)]
13. Wei, C.; Sun, R.; Jiang, Y.; Guo, X.; Ying, Y.; Wen, Y.; Yang, H.; Wu, Y. Protease-protection strategy combined with the SERS tags for detection of O-GlcNAc transferase activity. *Sens. Actuat. B Chem.* **2021**, *345*, 130410. [[CrossRef](#)]
14. Schuerle, S.; Dudani, J.S.; Christiansen, M.G.; Anikeeva, P.; Bhatia, S.N. Magnetically actuated protease sensors for in vivo tumor profiling. *Nano Lett.* **2016**, *16*, 6303–6310. [[CrossRef](#)] [[PubMed](#)]
15. Cheng, M.; Zhou, J.; Zhou, X.; Xing, D. Peptide cleavage induced assembly enables highly sensitive electrochemiluminescence detection of protease activity. *Sens. Actuat. B Chem.* **2018**, *262*, 516–521. [[CrossRef](#)]
16. Wignarajah, S.; Suaifan, G.A.R.Y.; Bizzarro, S.; Bikker, F.J.; Kaman, W.E.; Zourob, M. Colorimetric assay for the detection of typical biomarkers for periodontitis using a magnetic nanoparticle biosensor. *Anal. Chem.* **2015**, *87*, 12161–12168. [[CrossRef](#)] [[PubMed](#)]
17. Suaifan, G.A.R.Y.; Esseghaier, C.; Ng, A.; Zourob, M. Ultra-rapid colorimetric assay for protease detection using magnetic nanoparticle-based biosensors. *Analyst* **2013**, *138*, 3735–3739. [[CrossRef](#)]
18. Lee, G.-H.; Lee, E.J.; Hah, S.S. TAMRA- and Cy5-labeled probe for efficient kinetic characterization of caspase-3. *Anal. Biochem.* **2014**, *446*, 22–24. [[CrossRef](#)] [[PubMed](#)]
19. Vuojola, J.; Syrjänpää, M.; Lamminmäki, U.; Soukka, T. Genetically encoded protease substrate based on lanthanide-binding peptide for time-gated fluorescence detection. *Anal. Chem.* **2013**, *85*, 1367–1373. [[CrossRef](#)] [[PubMed](#)]
20. He, L.; Ye, S.; Fang, J.; Zhang, Y.; Cui, C.; Wang, A.; Zhao, Y.; Shi, H. Real-time visualization of embryonic apoptosis using a near-infrared fluorogenic probe for embryo development evaluation. *Anal. Chem.* **2021**, *93*, 12122–12130. [[CrossRef](#)]
21. den Hamer, A.; Dierickx, P.; Arts, R.; de Vries, J.S.P.M.; Brunsveld, L.; Merckx, M. Bright bioluminescent BRET sensor proteins for measuring intracellular caspase activity. *ACS Sens.* **2017**, *2*, 729–734. [[CrossRef](#)] [[PubMed](#)]
22. Yuan, Y.; Zhang, R.; Cheng, X.; Xu, S.; Liu, B. A FRET probe with AIEgen as the energy quencher: Dual signal turn-on for self-validated caspase detection. *Chem. Sci.* **2016**, *7*, 4245–4250. [[CrossRef](#)] [[PubMed](#)]
23. Cihlova, B.; Huskova, A.; Böserle, J.; Nencka, R.; Boura, E.; Silhan, J. High-throughput fluorescent assay for inhibitor screening of proteases from RNA viruses. *Molecules* **2021**, *26*, 3792. [[CrossRef](#)] [[PubMed](#)]
24. Su, J.; Rajapaksha, T.W.; Peter, M.E.; Mrksich, M. Assays of endogenous caspase activities: A comparison of mass spectrometry and fluorescence formats. *Anal. Chem.* **2006**, *78*, 4945–4951. [[CrossRef](#)] [[PubMed](#)]
25. Yang, Y.; Liang, Y.; Zhang, C. Label-free and homogenous detection of caspase-3-like proteases by disrupting homodimerization-directed bipartite tetracysteine display. *Anal. Chem.* **2017**, *89*, 4055–4061. [[CrossRef](#)]
26. Su, D.; Hu, X.; Dong, C.; Ren, J. Determination of Caspase 3 activity and its inhibition constant by combination of fluorescence correlation spectroscopy with a microwell chip. *Anal. Chem.* **2017**, *89*, 9788–9796. [[CrossRef](#)] [[PubMed](#)]
27. Zhou, J.; Cheng, M.; Zeng, L.; Liu, W.; Zhang, T.; Xing, D. Specific capture of the hydrolysate on magnetic beads for sensitive detecting plant vacuolar processing enzyme activity. *Biosens. Bioelectron.* **2016**, *79*, 881–886. [[CrossRef](#)] [[PubMed](#)]
28. Zhang, H.; Yu, D.; Zhao, Y.; Fan, A. Turn-on chemiluminescent sensing platform for label-free protease detection using streptavidin-modified magnetic beads. *Biosens. Bioelectron.* **2014**, *61*, 45–50. [[CrossRef](#)] [[PubMed](#)]
29. Liao, R.; Li, S.; Wang, H.; Chen, C.; Chen, X.; Cai, C. Simultaneous detection of two hepatocellular carcinoma-related microRNAs using a clever single-labeled fluorescent probe. *Anal. Chim. Acta* **2017**, *983*, 181. [[CrossRef](#)]
30. Wang, L.; Tian, J.; Li, H.; Zhang, Y.; Sun, X. A novel single-labeled fluorescent oligonucleotide probe for silver (I) ion detection based on the inherent quenching ability of deoxyguanosines. *Analyst* **2011**, *136*, 891–893. [[CrossRef](#)] [[PubMed](#)]
31. Deng, D.; Hao, Y.; Yang, P.; Xia, N.; Yu, W.; Liu, X.; Liu, L. Single-labeled peptide substrates for detection of protease activity based on the inherent fluorescence quenching ability of Cu²⁺. *Anal. Methods* **2019**, *11*, 1248–1253. [[CrossRef](#)]
32. Liu, L.; Zhang, H.; Wang, Z.; Song, D. Peptide-functionalized upconversion nanoparticles-based FRET sensing platform for caspase-9 activity detection in vitro and in vivo. *Biosens. Bioelectron.* **2019**, *141*, 111403. [[CrossRef](#)]
33. Yang, Y.; He, Y.; Deng, Z.; Li, J.; Huang, J.; Zhong, S. Intelligent nanoprobe: Acid-responsive drug release and in situ evaluation of its own therapeutic effect. *Anal. Chem.* **2020**, *92*, 12371–12378. [[CrossRef](#)]

34. Li, J.; Li, X.; Shi, X.; He, X.; Ma, N.; Chen, H. Highly sensitive detection of caspase-3 activities via a nonconjugated gold nanoparticle–quantum dot pair mediated by an inner-filter effect. *ACS Appl. Mater. Interfaces* **2013**, *5*, 9798–9802. [[CrossRef](#)] [[PubMed](#)]
35. Li, S.-Y.; Liu, L.-H.; Cheng, H.; Li, B.; Qiu, W.-X.; Zhang, X.-Z. A dual-FRET-based fluorescence probe for the sequential detection of MMP-2 and caspase-3. *Chem. Commun.* **2015**, *51*, 14520–14523. [[CrossRef](#)] [[PubMed](#)]
36. Jang, H.; Lee, J.; Min, D.-H. Graphene oxide for fluorescence-mediated enzymatic activity assays. *J. Mater. Chem. B* **2014**, *2*, 2452–2460. [[CrossRef](#)] [[PubMed](#)]
37. Lei, Z.; Jian, M.; Li, X.; Wei, J.; Meng, X.; Wang, Z. Biosensors and bioassays for determination of matrix metalloproteinases: State of the art and recent advances. *J. Mater. Chem. B* **2020**, *8*, 3261–3291. [[CrossRef](#)]
38. Nirantar, S.R.; Yeo, K.S.; Chee, S.; Lane, D.P.; Ghadessy, F.J. A generic scaffold for conversion of peptide ligands into homogenous biosensors. *Biosens. Bioelectron.* **2013**, *47*, 421–428. [[CrossRef](#)]
39. Xia, N.; Liu, G.; Yi, X. Surface plasmon resonance for protease detection by integration of homogeneous reaction. *Biosensors* **2021**, *11*, 362. [[CrossRef](#)] [[PubMed](#)]
40. Wang, M.; Lei, C.; Nie, Z.; Guo, M.; Huang, Y.; Yao, S. Label-free fluorescent detection of thrombin activity based on a recombinant enhanced green fluorescence protein and nickel ions immobilized nitrilotriacetic acid-coated magnetic nanoparticles. *Talanta* **2013**, *116*, 468–473. [[CrossRef](#)] [[PubMed](#)]
41. Wieneke, R.; Tamp, R. Multivalent chelators for in vivo protein labeling. *Angew. Chem. Int. Ed.* **2019**, *58*, 8278–8290. [[CrossRef](#)]
42. Wasserberg, D.; Cabanas-Danés, J.; Prangma, J.; O'Mahony, S.; Cazade, P.-A.; Tromp, E.; Blum, C.; Thompson, D.; Huskens, J.; Subramaniam, V.; et al. Controlling protein surface orientation by strategic placement of oligo-histidine tags. *ACS Nano* **2017**, *11*, 9068–9083. [[CrossRef](#)] [[PubMed](#)]
43. You, C.; Piehler, J. Multivalent chelators for spatially and temporally controlled protein functionalization. *Anal. Bioanal. Chem.* **2014**, *406*, 3345–3357. [[CrossRef](#)]
44. Mu, B.; Zhang, J.; McNicholas, T.P.; Reuel, N.F.; Kruss, S.; Strano, M.S. Recent advances in molecular recognition based on nanoengineered platforms. *Acc. Chem. Res.* **2020**, *47*, 979–988. [[CrossRef](#)] [[PubMed](#)]
45. Tateo, S.; Shintchi, H.; Matsumoto, H.; Nagata, N.; Hashimoto, M.; Wakao, M.; Suda, Y. Optimized immobilization of single chain variable fragment antibody onto non-toxic fluorescent nanoparticles for efficient preparation of a bioprobe. *Colloids Surf. B Biointerfaces* **2023**, *224*, 113192. [[CrossRef](#)] [[PubMed](#)]
46. Zhang, L.-S.; Yin, Y.-L.; Wang, L.; Xia, Y.; Ju Ryu, S.; Xi, Z.; Li, L.-Y.; Zhang, Z.-S. Self-assembling nitrilotriacetic acid nanofibers for tracking and enriching His-tagged proteins in living cells. *J. Mater. Chem. B* **2021**, *9*, 80–84. [[CrossRef](#)] [[PubMed](#)]
47. Lei, Q.; Huang, X.; Zheng, L.; Zheng, F.; Dong, J.; Chen, F.; Zeng, W. Biosensors for caspase-3: From chemical methodologies to biomedical applications. *Talanta* **2022**, *240*, 123198. [[CrossRef](#)] [[PubMed](#)]
48. Huang, R.; Wang, X.; Wang, D.; Liu, F.; Mei, B.; Tang, A.; Jiang, J.; Liang, G. Multifunctional fluorescent probe for sequential detections of glutathione and caspase 3 in vitro and in cells. *Anal. Chem.* **2013**, *85*, 6203–6207. [[CrossRef](#)] [[PubMed](#)]
49. Wang, M.; Li, L.; Zhang, L.; Zhao, J.; Jiang, Z.; Wang, W. Peptide-derived biosensors and their applications in tumor immunology-related detection. *Anal. Chem.* **2022**, *94*, 431–441. [[CrossRef](#)] [[PubMed](#)]
50. Chen, C.; La, M. Recent developments in electrochemical, electrochemiluminescent, photoelectrochemical methods for the detection of caspase-3 activity. *Int. J. Electrochem. Sci.* **2020**, *15*, 6852–6862. [[CrossRef](#)]
51. Hu, B.; Zhang, Q.; Gao, X.; Xu, K.; Tang, B. Monitoring the activation of caspases-1/3/4 for describing the pyroptosis pathways of cancer cells. *Anal. Chem.* **2021**, *93*, 12022–12031. [[CrossRef](#)] [[PubMed](#)]
52. Liu, X.; Song, X.; Luan, D.; Hu, B.; Xu, K.; Tang, B. Real-time in situ visualizing of the sequential activation of caspase cascade using a multicolor gold–selenium bonding fluorescent nanoprobe. *Anal. Chem.* **2019**, *91*, 5994–6002. [[CrossRef](#)]
53. Hu, X.; Li, H.; Huang, X.; Zhu, Z.; Zhu, H.; Gao, Y.; Zhu, Z.; Chen, H. Cell membrane-coated gold nanoparticles for apoptosis imaging in living cells based on fluorescent determination. *Microchim. Acta* **2020**, *187*, 175. [[CrossRef](#)] [[PubMed](#)]
54. Shi, Y.; Yi, C.; Zhang, Z.; Zhang, H.; Li, M.; Yang, M.; Yang, Q. Peptide-bridged assembly of hybrid nanomaterial and its application for caspase 3 detection. *ACS Appl. Mater. Interfaces* **2013**, *5*, 6494–6501. [[CrossRef](#)] [[PubMed](#)]
55. Wang, H.; Zhang, Q.; Chu, X.; Chen, T.; Ge, J.; Yu, R. Graphene oxide–peptide conjugate as an intracellular protease sensor for caspase-3 activation imaging in live cells. *Angew. Chem. Int. Ed.* **2011**, *50*, 7065–7069. [[CrossRef](#)]
56. Li, X.; Li, Y.; Qiu, Q.; Wen, Q.; Zhang, Q.; Yang, W.; Yuwen, L.; Weng, L.; Wang, L. Efficient biofunctionalization of MoS₂ nanosheets with peptides as intracellular fluorescent biosensor for sensitive detection of caspase-3 activity. *J. Colloid Interface Sci.* **2019**, *543*, 96–105. [[CrossRef](#)]
57. Dong, X.; Ong, S.Y.; Zhang, C.; Chen, W.; Du, S.; Xiao, Q.; Gao, L.; Yao, S.Q. Broad-spectrum polymeric nanoquencher as an efficient fluorescence sensing platform for biomolecular detection. *ACS Sens.* **2021**, *6*, 3102–3111. [[CrossRef](#)]
58. Shen, Y.; Xin, Z.; Zhu, Y.; Wang, J. Mesoporous carbon nanospheres featured multifunctional fluorescent nanoprobe: Simultaneous activation and tracing of caspase-3 involved cell apoptosis. *Sens. Actuat. B Chem.* **2022**, *358*, 131485. [[CrossRef](#)]
59. Xia, N.; Huang, Y.; Cui, Z.; Liu, S.; Deng, D.; Liu, L.; Wang, J. Impedimetric biosensor for assay of caspase-3 activity and evaluation of cell apoptosis using self-assembled biotin-phenylalanine network as signal enhancer. *Sens. Actuat. B Chem.* **2020**, *320*, 128436. [[CrossRef](#)]
60. Xia, N.; Sun, Z.; Ding, F.; Wang, Y.; Sun, W.; Liu, L. Protease biosensor by conversion of a homogeneous assay into a surface-tethered electrochemical analysis based on streptavidin-biotin interactions. *ACS Sens.* **2021**, *6*, 1166–1173. [[CrossRef](#)] [[PubMed](#)]

61. Vuojol, J.; Riuttamäki, T.; Kulta, E.; Arppe, R.; Soukka, T. Fluorescence-quenching-based homogeneous caspase-3 activity assay using photon upconversion. *Anal. Chim. Acta* **2012**, *725*, 67–73. [[CrossRef](#)] [[PubMed](#)]
62. Valanne, A.; Malmi, P.; Appelblom, H.; Niemelä, P.; Soukka, T. A dual-step fluorescence resonance energy transfer-based quenching assay for screening of caspase-3 inhibitors. *Anal. Biochem.* **2008**, *375*, 71–81. [[CrossRef](#)] [[PubMed](#)]

Disclaimer/Publisher’s Note: The statements, opinions and data contained in all publications are solely those of the individual author(s) and contributor(s) and not of MDPI and/or the editor(s). MDPI and/or the editor(s) disclaim responsibility for any injury to people or property resulting from any ideas, methods, instructions or products referred to in the content.